

2006-08-17

Functional interaction of the retinoblastoma and Ini1/Snf5 tumor suppressors in cell growth and pituitary tumorigenesis

Cynthia J. Guidi
University of Massachusetts Medical School

Et al.

Let us know how access to this document benefits you.

Follow this and additional works at: <https://escholarship.umassmed.edu/oapubs>



Part of the [Cancer Biology Commons](#), [Cell Biology Commons](#), and the [Medical Pathology Commons](#)

Repository Citation

Guidi CJ, Mudhasani RR, Hoover K, Koff A, Leav I, Imbalzano AN, Jones SN. (2006). Functional interaction of the retinoblastoma and Ini1/Snf5 tumor suppressors in cell growth and pituitary tumorigenesis. Open Access Articles. <https://doi.org/10.1158/0008-5472.CAN-06-1451>. Retrieved from <https://escholarship.umassmed.edu/oapubs/345>

This material is brought to you by eScholarship@UMMS. It has been accepted for inclusion in Open Access Articles by an authorized administrator of eScholarship@UMMS. For more information, please contact Lisa.Palmer@umassmed.edu.

Functional Interaction of the Retinoblastoma and *Ini1*/*Snf5* Tumor Suppressors in Cell Growth and Pituitary Tumorigenesis

Cynthia J. Guidi,¹ Rajini Mudhasani,¹ Kathleen Hoover,¹ Andrew Koff,⁴ Irwin Leav,² Anthony N. Imbalzano,¹ and Stephen N. Jones^{1,3}

Departments of ¹Cell Biology, ²Pathology, and ³Cancer Biology, University of Massachusetts Medical School, Worcester, Massachusetts and ⁴Department of Molecular Biology, Memorial Sloan-Kettering Cancer Center, New York, New York

Abstract

The *Ini1* subunit of the SWI/SNF chromatin remodeling complex suppresses formation of malignant rhabdoid tumors in humans and mice. Transduction of *Ini1* into *Ini1*-deficient tumor-derived cell lines has indicated that *Ini1* arrests cell growth, controls chromosomal ploidy, and suppresses tumorigenesis by regulating components of the retinoblastoma (Rb) signaling pathway. Furthermore, conditional inactivation of *Ini1* in mouse fibroblasts alters the expression of various Rb-E2F-regulated genes, indicating that endogenous *Ini1* levels may control Rb signaling in cells. We have reported previously that loss of one allele of *Ini1* in mouse fibroblasts results only in a 15% to 20% reduction in total *Ini1* mRNA levels due to transcriptional compensation by the remaining *Ini1* allele. Here, we examine the effects of *Ini1* haploinsufficiency on cell growth and immortalization in mouse embryonic fibroblasts. In addition, we examine pituitary tumorigenesis in Rb-*Ini1* compound heterozygous mice. Our results reveal that heterozygosity for *Ini1* up-regulates cell growth and immortalization and that exogenous *Ini1* down-regulates the growth of primary cells in a Rb-dependent manner. Furthermore, loss of *Ini1* is redundant with loss of Rb function in the formation of pituitary tumors in Rb heterozygous mice and leads to the formation of large, atypical Rb^{+/-} tumor cells lacking adrenocorticotrophic hormone expression. These results confirm *in vivo* the relationship between Rb and *Ini1* in tumor suppression and indicate that *Ini1* plays a role in maintaining the morphologic and functional differentiation of corticotrophic cells. (Cancer Res 2006; 66(16): 8076-82)

Introduction

SWI/SNF chromatin remodeling complexes hydrolyze ATP to alter nucleosome-DNA contacts to activate or repress eukaryotic gene expression (reviewed in refs. 1, 2). The subunit composition of SWI/SNF complexes varies among cell types; however, all human SWI/SNF complexes include either the catalytic ATPase subunit BRM (Brahma) or BRG1 (Brahma-related gene 1), as well as *Ini1* (3, 4). The *Ini1* subunit (also known as *Snf5*) was originally isolated as a cellular host protein that binds specifically to HIV-1 integrase and as a human homologue to the yeast *Snf5* component of yeast SWI/SNF complex (5, 6).

Chromosomal abnormalities at the *Ini1* locus have linked *Ini1* mutation with early childhood cancers. Known broadly as rhabdoid

predisposition syndrome, these cancers include atypical teratoid and rhabdoid tumors of the central nervous system and malignant rhabdoid tumors (MRT). Germ-line mutations in *Ini1* have been detected in MRT of the kidney and brain, with subsequent deletion or mutation of the wild-type (WT) *Ini1* allele in these tumors (7). Biallelic *Ini1* mutations have also been detected in sporadic renal rhabdoid tumors, choroid plexus carcinomas, medulloblastomas, and central primitive neuroectodermal tumors (8–10). The link between *Ini1* mutation and cancer and the loss of heterozygosity (LOH) for *Ini1* observed in human familial MRT strongly suggests that *Ini1* functions to suppress tumorigenesis.

The tumor-suppressing properties of *Ini1* were confirmed by studies of mice bearing mutations in *Ini1*. Embryos homozygous for disruption of *Ini1* (*Ini1*^{+/-}) fail to develop beyond the peri-implantation stage of gestation (11, 12). Mice haploinsufficient for *Ini1* (*Ini1*^{+/-}) develop normally, but approximately a quarter of these mice will develop rhabdoid tumors and undifferentiated sarcomas primarily on the head and neck, many of which are highly aggressive and metastatic (11–13). Further analysis indicated that tumor tissues showed loss of the remaining *Ini1* locus or were deficient for *Ini1* protein, confirming that the tumors underwent LOH for *Ini1* (11, 12). More recently, transient inactivation of *Ini1* using a reversible conditional *Ini1* allele in mice led to rapid bone marrow failure and death of the mice, whereas sporadic inactivation of *Ini1* in hematopoietic tissues and in other organs resulted in an extremely rapid onset of CD8⁺ lymphomas and rhabdoid tumors in all mice (14).

Reintroduction of *Ini1* into *Ini1*-deficient human tumor cell lines induces a G₁ arrest in these cells, a characteristic flat cell formation, and, in some cases, cell senescence or apoptosis (15–19). *Ini1*-deficient tumor cell lines also exhibit chromosomal instability and polyploidy, both of which can be restored to more normal conditions by transduction of *Ini1* (20). Recent work has begun to investigate the underlying mechanisms of *Ini1*-mediated effects on cell growth and tumor suppression. The SWI/SNF ATPase subunits BRG1 and BRM are implicated in control of cell growth and proliferation through their direct interaction with the retinoblastoma (Rb) tumor suppressor protein (21–24). Rb functions as a key regulator of the G₁-S transition during cell cycling by binding and inhibiting the activity of E2F transcription factors. Phosphorylation of Rb by cyclin-dependent kinases (CDK) interrupts Rb-E2F interactions, leading to E2F-induced expression of genes involved in DNA replication and progression of the cell cycle into S phase. The link between SWI/SNF ATPases and Rb has promoted investigations into the effects of *Ini1* loss on the Rb signaling pathway. Induction of Rb signaling was found to restore the G₁ arrest in *Ini1*-deficient cells, suggesting that *Ini1* acts upstream of Rb in regulating the G₁ checkpoint (16, 18). In support of this hypothesis, reintroduction of *Ini1* into MRT cells was reported to activate the CDK inhibitor p16^{INK4a} (25) and to induce senescence in cultured

Requests for reprints: Stephen N. Jones, Department of Cell Biology S3-214, University of Massachusetts Medical School, 55 Lake Avenue North, Worcester, MA 01655. Phone: 508-856-7500; Fax: 508-856-5612; E-mail: stephen.jones@umassmed.edu.
©2006 American Association for Cancer Research.
doi:10.1158/0008-5472.CAN-06-1451

rhabdoid cells by binding directly to the p16^{INK4a} and p21^{WAF/CIP} promoters and up-regulating the expression of these CDK inhibitors (26). In addition, exogenous Ini1 induces HDAC-dependent repression of the cyclin D1 promoter (17), and RNA interference inhibition of cyclin D1 activity was sufficient to restore a G₁ arrest and apoptosis in Ini1-deficient MRT cells (26). Finally, gene expression profiling indicates that Ini1 activates a mitotic checkpoint and ploidy control through regulation of E2F target genes (20).

These tumor cell-based studies suggest that Ini1 functions by altering CDK phosphorylation of the Rb tumor suppressor. Studies in *Drosophila* also implicate the Ini1 homologue Snr1 in controlling cell growth via the Rb-E2F pathway (27, 28). However, less evidence is available about the effects of Ini1 loss in normal mammalian cells. Very recently, Ini1 was conditionally deleted in mouse embryonic fibroblasts (MEF) by use of the Cre-lox system. In one report, loss of Ini1 led to aberrant regulation of certain E2F target genes whose expression levels are also altered in MRT cells. In addition, inactivation of Ini1 induced a G₂ cell cycle arrest, polyploidy, and apoptosis, with concomitant increases in levels of p53 and p21 (29). However, in another report, inactivation of Ini1 impaired cell proliferation and survival and induced p53 levels without affecting E2F-responsive genes (30). These data suggest that Ini1 loss may perturb both Rb and p53 tumor suppression pathways. Conditional inactivation of either Rb or p16^{INK4a} did not alter the rate of tumorigenesis in mice, in which Ini1 was also conditionally inactivated by induction of Cre expression from an MX1-Cre transgene (29), whereas coinactivation of both Ini1 and p53 led to a dramatic increase in the rate of tumor onset (29, 30). Therefore, apparently, mutation of Rb, but not p53, might be redundant with Ini1 loss of function *in vivo*.

We have generated previously Ini1-heterozygous mice and MEFs and observed that the Ini1 levels in these Ini1-haploinsufficient cells are similar to WT Ini1 levels due to an increase in the activity of the remaining Ini1 promoter (12, 31). However, this transcriptional compensation for loss of one allele of Ini1 is not complete and results in a 15% to 20% reduction in total Ini1 levels in the Ini1-heterozygous cells. Thus, individuals heterozygous for Ini1 may be susceptible to the consequences of reduced Ini1 levels. To better understand the functional relationship between Ini1 and the Rb tumor suppressor and to determine if haploinsufficiency of Ini1 is sufficient to alter cell growth, we examined the growth characteristics of Ini1-heterozygous MEFs. Our results indicate that haploinsufficiency of Ini1 increases the rate of cell proliferation and cell immortalization and that Ini1 requires functional Rb to induce a senescent-like phenotype in primary cells. Moreover, mice heterozygous for Rb or for both Rb and Ini1 form highly penetrant pituitary tumors at similar rates. Although adrenocorticotrophic hormone (ACTH)-positive tumor cells displaying LOH for the remaining WT Rb allele were present in tumors from both cohorts of mice, large atypical tumor cells lacking ACTH expression were also readily detected solely in pituitary tumors in the Rb^{+/-}, Ini1^{+/-} mice. Laser capture microdissection (LCM) revealed that the small, ACTH-positive cells underwent LOH for the WT Rb allele while retaining heterozygosity for Ini1, whereas the large atypical tumor cells underwent LOH for Ini1 but not for Rb. These findings indicate that Ini1 and Rb have redundant functions in suppressing pituitary tumorigenesis in Rb-heterozygous mice and that Ini1 is important for maintaining the morphologic and functional differentiation of normal corticotrophic cells as well as those undergoing neoplastic transformation.

Materials and Methods

Cells and mice. Ini1-heterozygous mice and Rb-heterozygous mice have been described previously (12, 32). MEFs were generated from E12 to E14 embryos as described (33). Genomic DNA was prepared from the hind limb of each embryo for PCR analysis to identify the genotype of the resulting fibroblast line. All studies were initiated using low-passage embryonic fibroblasts (passages 2-4). Ini1^{+/-}, Rb^{+/-}, and Ini1^{+/-}, Rb^{+/-} mice were maintained on a C57Bl/6×129 genetic background. All mice were maintained and used in accordance with the University of Massachusetts Animal Care and Use Committee.

Cell studies. To determine the rates of cell proliferation, three different lines of WT MEF or Ini1-heterozygous MEFs were plated at 5×10^5 cells per 10-cm dish in MEF media (DMEM, with 10% fetal bovine serum, 0.37% sodium bicarbonate, penicillin, and streptomycin). Triplicate plates of cells for each line were harvested and counted at various times following initial plating using a Z1 Coulter Particle Counter (Beckman Coulter, Miami, FL). A 3T9 assay was done as described (34) to examine the rate of spontaneous immortalization of WT MEF and Ini1-heterozygous MEFs. Briefly, 3×10^6 cells were plated into MEF media in 10-cm dish every 3 days. A total of three plates (9×10^6 cells) were maintained for two separate lines of fibroblasts for each genotype. Triplicate plates for each line were trypsinized and mixed before counting and replating. Recombinant Ini1 retrovirus was generated as described previously (31) and used to transduce Ini1 into WT and Rb-null MEFs. Cells were plated onto 10-cm dishes in MEF media at 5×10^5 per plate and infected with either an Ini1-flag recombinant retrovirus or an empty vector recombinant virus for 24 hours in the presence of polybrene. Infected cells were transiently selected in blasticidin (10 µg/mL) for 60 hours to identify cells transduced by the recombinant Ini1 virus, harvested by trypsinization, and counted. Triplicate platings of transduced cells for each genotype were replated at a density of 4×10^4 cells per 10-cm dish, and plates were harvested at various time points following initial plating and counted using a Z1 Coulter Particle Counter.

Reverse transcription-PCR to detect Ini1 transcripts. Reverse transcription-PCR (RT-PCR) was done on reverse-transcribed total RNA isolated from MEFs infected with either pBABE-flag-Ini1 or pBABE-no insert (31). The primers for the flag-Ini1 cDNA were 5'-GTCACCACCATCG-CATACAG-3' (F922) and 5'-TCATTATTGTGCATCGTCGCTT-3' (R1188). The primers for the 36B4 control cDNA were 5'-CAGGCCCTGCACTC-TCGCTTCTG-3' (F699) and 5'-TTGGTTGCTTGGCGGGATTAGTC-3' (R1023).

Western analysis. Protein was extracted from 3T9 cells at various passages and quantified by Bradford analysis, and 50 µg of each sample were used for Western analysis with an Ini1 antibody as described (12).

Tumor assays. Ini1-heterozygous mice were crossed with Rb heterozygous mice to establish a cohort of Rb-Ini1 compound heterozygous mice. Tumor assays were done using these mice and Rb heterozygous mice. Mice were inspected every other day for morbidity or tumor formation. Necropsies were done and tumors were harvested and fixed in 10% buffered formalin phosphate and then processed for paraffin embedding and sectioning using standard methods. Sections were mounted on a glass slide and stained with H&E. Sections of adenomas and normal pituitaries from WT mice were also immunostained for ACTH. Before LCM, coverslipped, H&E-stained, and ACTH-immunostained sections were studied microscopically. Areas of interest were then identified in replicate deparaffinized, noncovered sections, and LCM was done using an Arcturus (Mountain View, CA) Pixcell 2 instrument.

Genotyping of tumor samples. Following microdissection of select areas of tumor slides, the samples were placed into a small Eppendorf tube and genotyped by PCR for Ini1 and Rb status as described previously (12, 32).

Results

Increased proliferation of Ini1-heterozygous fibroblasts. Multiple lines of Ini1^{+/-} MEFs or WT MEFs were generated by standard methods from E13.5 embryos isolated from pregnant

$Ini1^{+/-}$ female mice intercrossed with WT male mice. Three separate lines of $Ini1^{+/-}$ or WT MEFs were harvested, plated, and counted at various times after initial plating to characterize the growth rate of these early-passage fibroblasts. The results indicate that $Ini1^{+/-}$ primary fibroblasts show an increase in their rate of proliferation relative to WT fibroblasts (Fig. 1A). This assay was repeated twice with similar results.

Cell immortalization studies. To explore the effects of $Ini1$ haploinsufficiency on cell immortalization, we did a 3T9 assay on two lines each of MEFs that were either WT or heterozygous for $Ini1$ (Fig. 1B). WT MEFs failed to immortalize during the course of this 3T9 assay, whereas MEFs that were $Ini1^{+/-}$ underwent rapid spontaneous immortalization by the fifth passage. Western analysis of $Ini1^{+/-}$ MEFs at various passages during the 3T9 assay revealed that these cells did not require $Ini1$ LOH to immortalize, as $Ini1$ expression was detected throughout various time points in $Ini1^{+/-}$ cells during the course of the 3T9 assay, including as late as passage 30 (Fig. 1C).

Cell transduction studies. Forced overexpression of $Ini1$ in MRT cells induces a flattened cell morphology and reduced cell growth, and several reports have implicated involvement of the Rb signaling pathway in $Ini1$ -induced senescence (19, 26). To document the role of Rb in primary cells in $Ini1$ -mediated cell senescence, we infected multiple lines of WT MEFs or MEFs derived from Rb-null embryos with a recombinant retrovirus that encodes a flag-tagged $Ini1$ and a blasticidin drug selection marker. Following infection and transient selection in blasticidin, the cells were harvested and plated in 10-cm dishes, and a proliferation assay was done using the transduced cells (35). WT MEFs infected with an empty vector virus continued to proliferate slowly throughout the assay (Fig. 2A). In contrast, WT MEFs transduced with virus encoding $Ini1$ assumed a flattened

cell appearance and divided only minimally postinfection. As expected, Rb-null MEFs infected with an empty vector proliferated far faster than WT MEFs infected with empty vector virus. Interestingly, transduction of $Ini1$ failed to alter the morphology or growth characteristics of Rb-null MEFs, indicating that the replicative senescence-like effects of $Ini1$ expression are Rb-dependent. RT-PCR analysis of total RNA harvested from mock or $Ini1$ -transduced cells confirmed expression of exogenous, flag-tagged $Ini1$ in Rb and WT MEFs infected with the recombinant $Ini1$ virus (Fig. 2B).

Tumorigenesis in $Ini1$ -Rb compound heterozygous mice. We have described previously $Ini1$ as a tumor suppressor in mice (12). To explore further genetic interactions between the $Ini1$ and Rb tumor suppressors *in vivo*, we generated Rb- $Ini1$ compound heterozygous mice by breeding $Ini1^{+/-}$ mice with $Rb^{+/-}$ mice. Rb-null mice develop normally until E14 but fail to develop thereafter due to massive cell death in the nervous system and defects in erythropoiesis (32, 36, 37). $Rb^{+/-}$ mice are viable and appear normal but form foci of atypical melanotroph precursor cells in the intermediate lobe of the pituitary as early as 30 days after birth (38). Eventually, adenocarcinomas develop in the anterior pituitary lobe as do medullary thyroid adenomas and neuroendocrine tumors (38–41). Ultimately, 100% of $Rb^{+/-}$ mice succumb to pituitary tumors, and LOH for the WT Rb allele is observed in all late-stage tumors and in some of the microdissected atypical cells of early proliferates (38, 40).

To determine whether haploinsufficiency for $Ini1$ alters tumorigenesis in Rb heterozygous mice, a cohort of $Rb^{+/-}$, $Ini1^{+/-}$ mice was generated and analyzed for the formation of spontaneous tumors. The rate and tissue spectrum of tumor formation in these compound heterozygous mice was compared with tumorigenesis in mice heterozygous for either Rb or $Ini1$. Mice heterozygous for

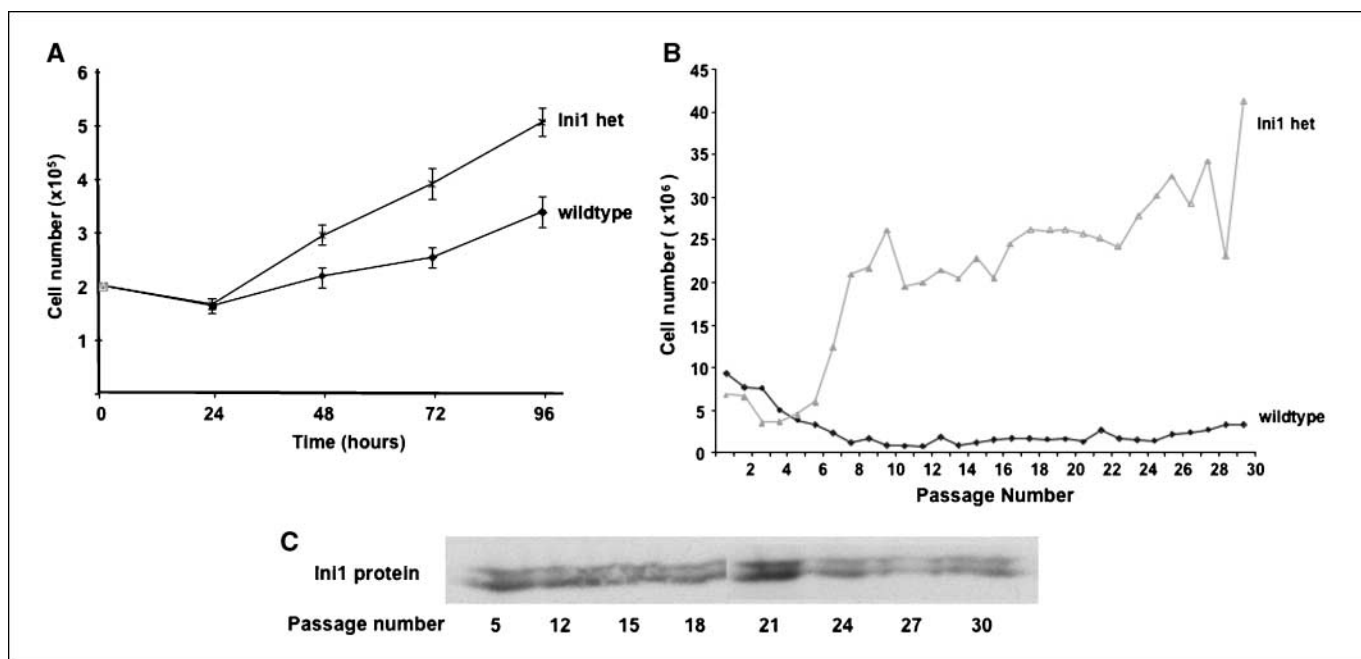


Figure 1. Haploinsufficiency for $Ini1$ alters the proliferation and spontaneous immortalization of MEFs. **A**, analysis of the growth rate of (WT) MEFs and $Ini1$ -heterozygous MEFs reveals that $Ini1$ haploinsufficiency induces a faster rate of proliferation in cells. **B**, immortalization of WT MEFs and $Ini1$ -heterozygous MEFs. WT MEFs failed to immortalize following a 3T9 protocol to assess spontaneous immortalization, whereas cells haploinsufficient for $Ini1$ readily immortalized. **C**, Western analysis of $Ini1$ protein in the immortalized $Ini1^{+/-}$ cells at various passage numbers reveals that the $Ini1$ -heterozygous cells retain $Ini1$ expression. The $Ini1$ antibody detects two $Ini1$ proteins generated through differential splicing of the $Ini1$ transcript (50).

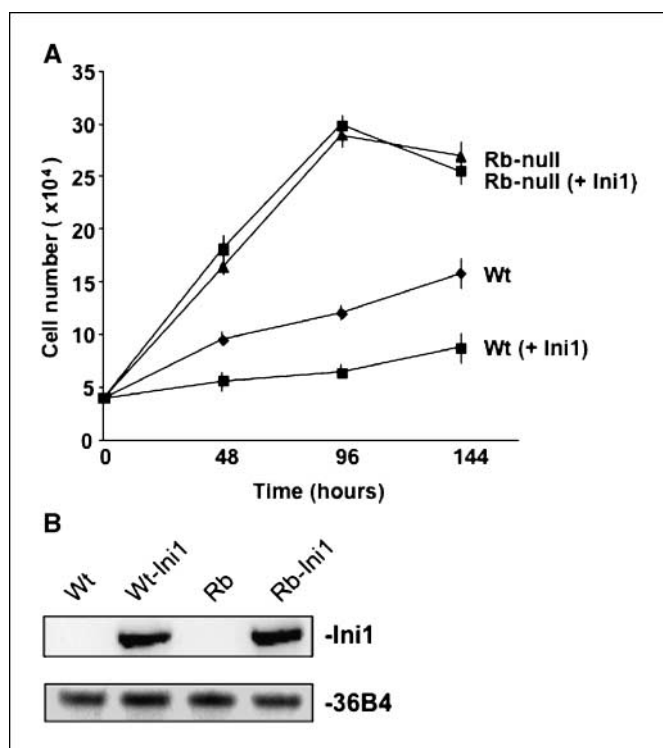


Figure 2. Overexpression of *Ini1* in MEFs induces cell growth arrest. **A**, retroviral-mediated transduction of *Ini1* into WT MEFs retards the growth of these cells and induces a senescence-like state. However, transduction of *Ini1* into Rb-null MEFs does not alter the growth of these cells, showing that effects of *Ini1* overexpression on cell growth are Rb-dependent. **B**, transduced *Ini1* (flag-tag) expression is detected by RT-PCR using primers to *Ini1* and the flag sequences in WT and Rb^{+/-} MEFs infected with *Ini1* recombinant retrovirus. RT-PCR against 36B4 cDNA was done as a control for RNA quality.

both Rb and *Ini1* developed pituitary tumors at a rate and penetrance indistinguishable from tumor formation in Rb^{+/-} mice (Fig. 3). The spectrum of tumors observed in Rb^{+/-} mice WT or heterozygous for *Ini1* was also quite similar; except for one compound heterozygous mouse that developed thymic lymphoma, only pituitary tumorigenesis was detected Rb^{+/-} mice and in Rb^{+/-}, *Ini1*^{+/-} mice. Interestingly, no rhabdoid-like tumors or poorly differentiated sarcomas were observed on the head and neck of *Ini1*^{+/-}, Rb^{+/-} mice during this assay, although ~20% of *Ini1*^{+/-} mice present with these cancers in the same time frame. Thus, haploinsufficiency for *Ini1* does not alter the onset, penetrance, or spectrum of tumor formation in Rb^{+/-} mice. Furthermore, deletion of WT Rb or WT *Ini1* did not rescue the embryonic lethality of either *Ini1*-null mice or Rb-null mice, respectively, because intercrossing of the compound heterozygous mice did not cause *Ini1*-null or Rb-null mice.

Histologic features and genotype of tumors arising in Rb^{+/-}, Ini1^{+/-} mice. The size of pituitary tumors in the Rb-*Ini1* compound heterozygous mice ranged from 4 to 7 mm in diameter, similar to what was observed in pituitary tumors arising in Rb^{+/-} mice in this and in other published studies (39, 42).

Pituitary tumors in Rb^{+/-} mice contained a uniform population of cells that morphologically resemble corticotrophic cells normally present in the intermediate and anterior pituitary lobes. Analysis of tumor sections revealed that the tumor cells in the pituitary of Rb heterozygous mice consistently immunostained strongly for ACTH (Fig. 4A). ACTH is a marker for anterior lobe

corticotrope pituitary cells (Fig. 4B) and is expressed in both benign and malignant pituitary tumors that arise in Rb^{+/-} mice (43).

Tumors from Rb^{+/-}, *Ini1*^{+/-} compound mice also exhibited a similar morphology and robust ACTH staining pattern. However, large ACTH-negative cells could also be found in more than half of the Rb^{+/-}, *Ini1*^{+/-} tumors. These atypical cells were usually polygonal, displayed large round vesicular nuclei, and abundant amphophilic cytoplasm and present in aggregates scattered throughout the tumor tissue (Fig. 4C-D). Notably, these large ACTH-negative cells were observed only in pituitary tumors that arose in the Rb-*Ini1* compound heterozygous mice.

Laser capture microscopy was done on sections of several different pituitary tumors that arose in Rb-heterozygous mice to genotype the small typical cells present in the tumor mass (Fig. 5A). In each case, the cells had undergone LOH for the WT Rb allele in the tumor (Fig. 5B), consistent with previous reports on pituitary tumorigenesis in Rb-heterozygous mice (38, 40). The presence of atypical cells in the compound heterozygous tumors prompted us to examine whether the cells bearing these unique features had undergone LOH for the WT *Ini1* allele. Cells from regions of tumors that contained the large, ACTH-negative cells were collected by laser capture microscopy, as were small cells from regions bearing the classic features of typical Rb^{+/-} pituitary adenomas. In three of four Rb^{+/-}, *Ini1*^{+/-} tumors examined, the large atypical cells displayed loss of the WT *Ini1* allele. In marked contrast, the WT *Ini1* allele was retained in the smaller cells from the same tumors (Fig. 5C and D). Previous studies of pituitary adenomas in Rb^{+/-} mice showed for the WT Rb allele in both earliest detected atypical proliferates and all pituitary adenocarcinomas. However, genotyping of the large, ACTH-negative cells present in the pituitary tumors of Rb-*Ini1* compound heterozygous mice in this present study revealed that the WT Rb allele was retained in the large tumor cells. Instead, these atypical cells had undergone LOH for the functional *Ini1* allele.

Discussion

Evidence in the literature indicates that the *Ini1* tumor suppressor plays a role in regulating cell growth and chromosomal

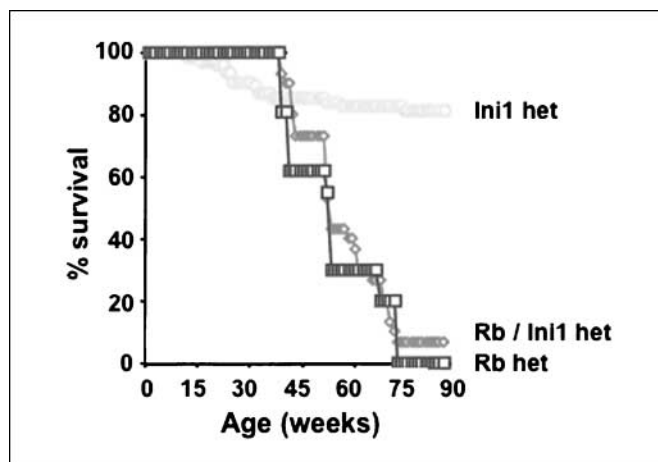


Figure 3. Interaction between Rb and *Ini1* in tumor suppression. **A** Kaplan-Meier plot of the frequency of spontaneous tumorigenesis in cohorts of *Ini1*^{+/-} (*Ini1* het), Rb^{+/-} (*Rb* het), or Rb^{+/-}, *Ini1*^{+/-} (*Rb/Ini1* het) mice (n = 25). Rb^{+/-} and Rb^{+/-}, *Ini1*^{+/-} mice succumbed to pituitary tumors at the same rate.

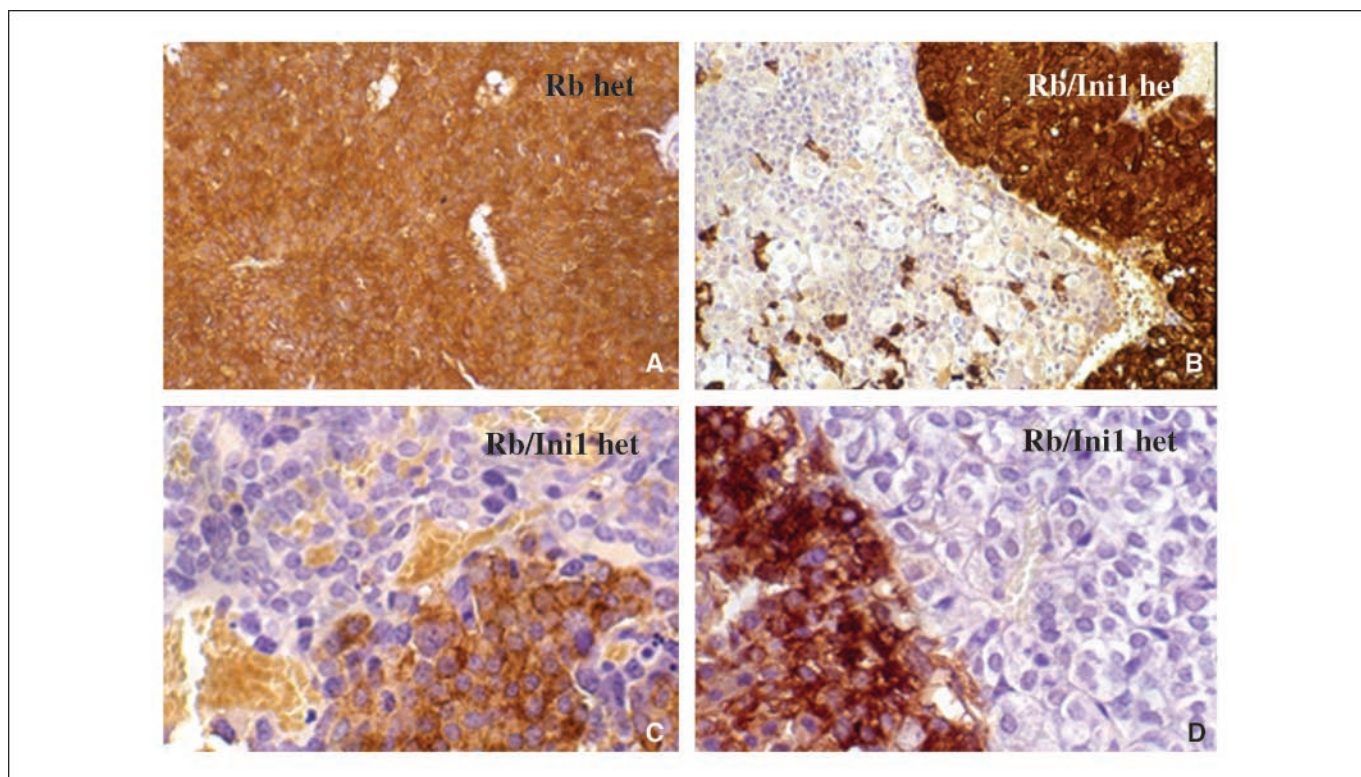


Figure 4. Identifying corticotropic tumor cells by immunostaining for ACTH. Although pituitary tumors formed in both cohorts of $Rb^{+/-}$ mice and in $Rb-Ini1^{+/-}$ mice, differences were seen in ACTH expression in the tumors. *A*, representative ACTH immunostaining of tumor cells in the pituitary of an $Rb^{+/-}$ mouse. All tested tumors that arose in $Rb^{+/-}$ mice stained highly for ACTH. *B*, ACTH staining in nontumor (control) pituitary tissue of $Rb^{+/+}$, $Ini1^{+/-}$ mice. ACTH is expressed in the intermediate lobe, with scattered foci of ACTH-positive cells in the adjacent anterior pituitary. *C* and *D*, non-ACTH cells were readily observed in tumors that formed in $Rb^{+/-}$, $Ini1^{+/-}$ mice. Non-ACTH staining cells were observed both in clusters within the tumor and in individual cells dispersed throughout the tumor sections.

ploidy by regulating components of the Rb signaling pathway, including CDK inhibitors and/or cyclin D1 (reviewed in ref. 44). However, most of these studies were done using forced overexpression of *Ini1* into *Ini1*-deficient malignant rhabdoid tumor-derived cell lines. More recently, analysis of tumorigenesis in mice revealed tumorigenesis induced by deletion of *Ini1* was not altered on codeletion of either *Rb* or $p16^{ink4}$, whereas loss of cyclin D1 activity inhibited tumorigenesis in *Ini1*-null mice (29, 45). These findings suggest that the *Rb* and *Ini1* may possess redundant tumor-suppressing capabilities. Less data are available about the role of *Ini1* in regulating p53 functions in cells or mice. Conditional deletion of *Ini1* was reported to increase p53 activity in MEFs, suggesting that *Ini1* negatively regulates p53 functions (29, 30). However, deletion of p53 also dramatically increased the onset of tumor formation following conditional deletion of *Ini1* in mice in these studies, suggesting that *Ini1* and p53 may also cooperate in preventing oncogenesis.

In this study, we have examined the growth characteristics of *Ini1*-haploinsufficient MEFs. The results reveal that loss of one allele of *Ini1* increases the rate of cell proliferation, in keeping with the findings of earlier reports, indicating that *Ini1* overexpression negatively regulates cell growth (15–19, 31). These data also indicate that haploinsufficiency of *Ini1* can have functional ramifications on cell proliferation despite the compensatory effects of increased *Ini1* expression from the remaining WT *Ini1* allele (31). Spontaneous immortalization of $Ini1^{+/-}$ MEFs was also readily achieved in the 3T9 assay. Interestingly,

cells haploinsufficient for *Ini1* spontaneously immortalized without undergoing loss for *Ini1*, whereas WT cells failed to immortalize in this assay, again suggesting that primary cells haploinsufficient for *Ini1* have altered growth characteristics.

To explore the *Rb*-mediated effects of *Ini1* in primary cells, we transduced *Ini1* expression into WT and *Rb*-deficient MEFs. Expression of exogenous *Ini1* in MEFs induced a cell growth arrest and flat cell morphology, similar to previous findings of the effect of forced *Ini1* expression in MRT cells (15–19). However, *Ini1* transduction had no effect on MEFs lacking functional *Rb*, indicating that the senescence-inducing properties of *Ini1* are *Rb*-dependent in these cells.

The development of pituitary adenomas in $Rb^{+/-}$ mice was accelerated on crossing the *Rb*-mutant mice with mice deficient for p27, p53, or $p19^{ARF}$ tumor suppressors (46–48). However, LOH of the WT *Rb* allele was observed in all tumors arising in these studies. To explore further the relationship between *Rb* and the *Ini1* tumor suppressor *in vivo*, we generated *Ini1-Rb* compound heterozygous mice and compared tumor formation in these mice with tumorigenesis in $Ini1^{+/-}$ or $Rb^{+/-}$ mice. The rate and spectrum of tumor formation in *Rb*-heterozygous mice was unaltered by the presence of one or two copies of functional *Ini1*. Analysis of the genotypes of tumor cells determined that most tumor cells displayed LOH for the WT *Rb* allele as expected. However, not all pituitary adenoma cells lost functional *Rb*: the large atypical cells that were ACTH negative retained the WT *Rb* allele and displayed LOH for the functional *Ini1* allele. These results indicate that loss of *Rb* or *Ini1* is redundant in

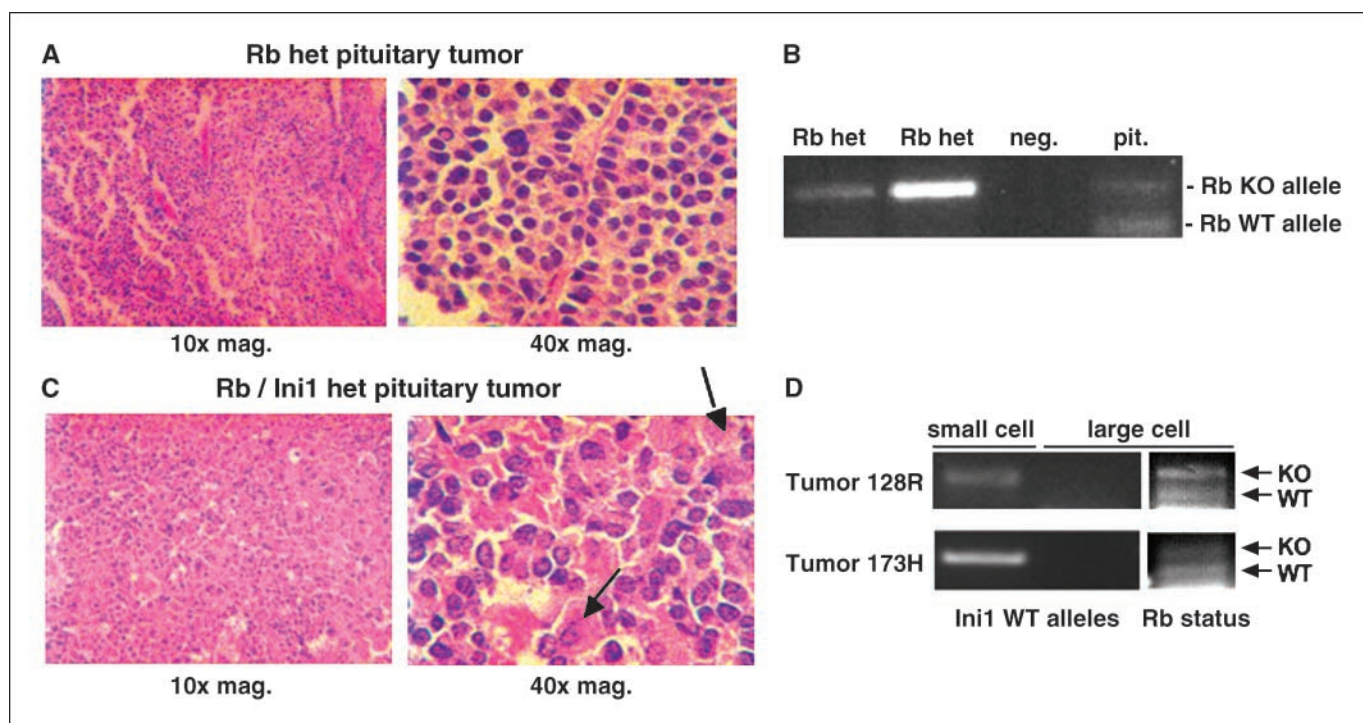


Figure 5. Tumors in $Rb^{+/-}$, $Ini1^{+/-}$ mice undergo LOH for either Rb or *Ini1*. *A*, typical H&E-stained section of a pituitary tumor that arose in a Rb-heterozygous mouse. Magnification of the image was either at $\times 10$ or $\times 40$. *B*, single cells were isolated from unstained tumor sections by laser capture microscopy, and DNA was isolated and used in PCRs to genotype the tumor. Two tumors that arose in $Rb^{+/-}$ mice displaying LOH for the WT Rb allele are shown, along with a negative control and a positive control (cells harvested from WT pituitary tissue). *C*, representative H&E-stained section of pituitary tumors that arose in *Ini1/Rb* compound heterozygous mouse. Magnification of the image was either at $\times 10$ or $\times 40$. Arrows, large, atypical tumor cell morphology that fail to express ACTH. *D*, examples of the genotyping of the atypical (large cells) and typical (small cells) found in the pituitary tumors of compound heterozygous mice. The large, ACTH-negative cells retained the WT Rb allele and underwent LOH for *Ini1*, whereas the smaller cells that stain for ACTH in the tumor mass also retain the functional *Ini1* allele and display LOH for Rb.

some pituitary tumors in mice, suggesting that these two tumor suppressors function similarly in preventing this type of cancer. However, loss of *Ini1* in these tumors also seemed to alter the morphology of the tumor cell, with *Ini1*-null cells appearing larger and lacking ACTH expression. Based on these observations, we hypothesize that loss of Rb or *Ini1* occurs early in cells of the intermediate and anterior pituitary lobes in the $Ini1^{+/-}$. $Rb^{+/-}$ mice and that complete loss of one tumor suppressor eliminates the need for LOH of the other suppressor gene in tumor formation. Surprisingly, mice haploinsufficient for both Rb and *Ini1* failed to form any sarcomas or rhabdoid-like tumors of the head and neck in contrast to those observed in $Ini1^{+/-}$ mice. Therefore, although Rb and *Ini1* appear redundant in suppressing pituitary tumorigenesis in these mice, the lack of MRT tumors in the $Rb^{+/-}$, $Ini1^{+/-}$ mice suggests that Rb is epistatic to *Ini1* in tumor suppression.

The appearance of *Ini1*-deficient pituitary tumor cells that were enlarged relative to the *Ini1* heterozygous, Rb-deficient tumor cells is reminiscent of the behavior of proliferating immortalized cells that express a dominant-negative version of the Brg1 ATPase. These cells were larger than counterpart cells not expressing the mutant Brg1, showing increased area of surface attachment, increased cell volume, and increased levels of proteins associated with cell adhesion (49). In both studies, the results suggest that interference with SWI/SNF enzyme function affects pathways controlling cell size and shape without blocking cell proliferation. Additional analyses will be needed to identify the specific genes involved and to address mechanisms by which

chromatin remodeling enzymes affect the physical variables controlling cell size and shape. We note that these observations differ from previous documentation of a “flat cell” phenotype when *Ini1* or BRG1 are ectopically expressed in *Ini1*- or BRG1-deficient tumor cells (15–19, 21, 22), as these cells are inevitably growth arrested.

The results of our study indicate that *Ini1* regulates Rb functions in murine primary cells *in vitro* and *in vivo* and that *Ini1* haploinsufficiency has functional consequences on cell growth. These results suggest that there might be clinical ramifications to *Ini1* haploinsufficiency in members of MRT families. In addition, *Ini1* seems to have morphologic consequences in pituitary cells and to regulate ACTH expression. Further analysis of Rb functions in $Ini1^{+/-}$ and *Ini1*-null cells and in mice should help elucidate the precise interplay of these signaling pathways in regulating cell proliferation and in tumor suppression.

Acknowledgments

Received 4/21/2006; revised 6/8/2006; accepted 6/19/2006.

Grant support: National Institute of Diabetes and Digestive and Kidney Diseases Program Project grant 5P30DK32520 (core facilities) and NIH grants GM56244 (A.N. Imbalzano) and CA95216 (S.N. Jones).

The costs of publication of this article were defrayed in part by the payment of page charges. This article must therefore be hereby marked *advertisement* in accordance with 18 U.S.C. Section 1734 solely to indicate this fact.

We thank Dr. Michael Slayter of IDEXX Laboratories (Grafton, MA) for assistance in tumor analysis, Debra Rigor and Judith Gallant for technical assistance, Charlene Baron for help with article preparation, and Karen Dressler for assistance with ACTH immunostaining.

References

1. Smith CL, Peterson CL. ATP-dependent chromatin remodeling. *Curr Top Dev Biol* 2005;65:115–48.
2. Sif S. ATP-dependent nucleosome remodeling complexes: enzymes tailored to deal with chromatin. *J Cell Biochem* 2004;91:1087–98.
3. Kwon H, Imbalzano AN, Khavari PA, et al. Nucleosome disruption and enhancement of activator binding by a human SWI/SNF complex. *Nature* 1994;370:477–81.
4. Wang W, Cote J, Xue Y, et al. Purification and biochemical heterogeneity of the mammalian SWI-SNF complex. *EMBO J* 1996;15:5370–82.
5. Kalpana GV, Marmon S, Wang W, et al. Binding and stimulation of HIV-1 integrase by a human homolog of yeast transcription factor SNF5. *Science* 1994;266:2002–6.
6. Muchardt C, Sardet C, Bourachot B, et al. A human protein with homology to *Saccharomyces cerevisiae* SNF5 interacts with the potential helicase hbrm. *Nucleic Acids Res* 1995;23:1127–32.
7. Versteeg I, Sevenet N, Lange J, et al. Truncating mutations of hSNF5/INI1 in aggressive paediatric cancer. *Nature* 1998;394:203–6.
8. Rousseau-Merck MF, Versteeg I, Legrand I, et al. hSNF5/INI1 inactivation is mainly associated with homozygous deletions and mitotic recombinations in rhabdoid tumors. *Cancer Res* 1999;59:3152–6.
9. Sevenet N, Sheridan E, Amram D, et al. Constitutional mutations of the hSNF5/INI1 gene predispose to a variety of cancers. *Am J Hum Genet* 1999;65:1342–8.
10. Biegel JA, Kalpana G, Knudsen ES, et al. The role of INI1 and the SWI/SNF complex in the development of rhabdoid tumors: meeting summary from the workshop on childhood atypical teratoid/rhabdoid tumors. *Cancer Res* 2002;62:323–8.
11. Klochendler-Yeivin A, Fiette L, Barra J, et al. The murine SNF5/INI1 chromatin remodeling factor is essential for embryonic development and tumor suppression. *EMBO Rep* 2000;1:500–6.
12. Guidi CJ, Sands AT, Zambrowicz BP, et al. Disruption of Ini1 leads to peri-implantation lethality and tumorigenesis in mice. *Mol Cell Biol* 2001;21:3598–603.
13. Roberts CW, Galusha SA, McMenamin ME, et al. Haploinsufficiency of Snf5 (integrase interactor 1) predisposes to malignant rhabdoid tumors in mice. *Proc Natl Acad Sci U S A* 2000;97:13796–800.
14. Roberts CW, Leroux MM, Fleming MD, et al. Highly penetrant, rapid tumorigenesis through conditional inversion of the tumor suppressor gene Snf5. *Cancer Cell* 2002;2:415–25.
15. Ae K, Kobayashi N, Sakuma R, et al. Chromatin remodeling factor encoded by ini1 induces G₁ arrest and apoptosis in ini1-deficient cells. *Oncogene* 2002;21:3112–20.
16. Versteeg I, Medjkane S, Rouillard D, et al. A key role of the hSNF5/INI1 tumour suppressor in the control of the G₁-S transition of the cell cycle. *Oncogene* 2002;21:6403–12.
17. Zhang ZK, Davies KP, Allen J, et al. Cell cycle arrest and repression of cyclin D1 transcription by INI1/hSNF5. *Mol Cell Biol* 2002;22:5975–88.
18. Betz BL, Strobeck MW, Reisman DN, et al. Re-expression of hSNF5/INI1/BAF47 in pediatric tumor cells leads to G₁ arrest associated with induction of p16^{INK4a} and activation of RB. *Oncogene* 2002;21:5193–203.
19. Reincke BS, Rosson GB, Oswald BW, et al. INI1 expression induces cell cycle arrest and markers of senescence in malignant rhabdoid tumor cells. *J Cell Physiol* 2003;194:303–13.
20. Vries RG, Bezrookove V, Zuijderduijn LM, et al. Cancer-associated mutations in chromatin remodeler hSNF5 promote chromosomal instability by compromising the mitotic checkpoint. *Genes Dev* 2005;19:665–70.
21. Dunaief JL, Strober BE, Guha S, et al. The retinoblastoma protein and BRG1 form a complex and cooperate to induce cell cycle arrest. *Cell* 1994;79:119–30.
22. Strober BE, Dunaief JL, Guha S, et al. Functional interactions between the hBRM/hBRG1 transcriptional activators and the pRB family of proteins. *Mol Cell Biol* 1996;16:1576–83.
23. Zhang HS, Gavin M, Dahiya A, et al. Exit from G₁ and S phase of the cell cycle is regulated by repressor complexes containing HDAC-Rb-hSWI/SNF and Rb-hSWI/SNF. *Cell* 2000;101:79–89.
24. Strobeck MW, Knudsen KE, Fribourg AF, et al. BRG-1 is required for RB-mediated cell cycle arrest. *Proc Natl Acad Sci U S A* 2000;97:7748–53.
25. Oruetxebarria I, Venturini F, Kekalainen T, et al. p16^{INK4a} is required for hSNF5 chromatin remodeler-induced cellular senescence in malignant rhabdoid tumor cells. *J Biol Chem* 2004;279:3807–16.
26. Chai J, Charboneau AL, Betz BL, et al. Loss of the hSNF5 gene concomitantly inactivates p21^{CIP/WAF1} and p16^{INK4a} activity associated with replicative senescence in A204 rhabdoid tumor cells. *Cancer Res* 2005;65:10192–8.
27. Brumby AM, Zrally CB, Horsfield JA, et al. *Drosophila* cyclin E interacts with components of the Brahma complex. *EMBO J* 2002;21:3377–89.
28. Zrally CB, Marena DR, Dingwall AK. SNR1 (INI1/SNF5) mediates important cell growth control functions of the *Drosophila* Brahma (SWI/SNF) chromatin remodeling complex. *Genetics* 2004;168:199–214.
29. Isakoff MS, Sansam CG, Tamayo P, et al. Inactivation of the Snf5 tumor suppressor stimulates cell cycle progression and cooperates with p53 loss in oncogenic transformation. *Proc Natl Acad Sci U S A* 2005;102:17745–50.
30. Klochendler-Yeivin A, Picarsky E, Yaniv M. Increased DNA damage sensitivity and apoptosis in cells lacking the Snf5/Ini1 subunit of the SWI/SNF chromatin remodeling complex. *Mol Cell Biol* 2006;26:2661–74.
31. Guidi CJ, Veal TM, Jones SN, et al. Transcriptional compensation for loss of an allele of the Ini1 tumor suppressor. *J Biol Chem* 2004;279:4180–5.
32. Jacks T, Fazeli A, Schmitt EM, et al. Effects of an Rb mutation in the mouse. *Nature* 1992;359:295–300.
33. Todaro GJ, Green H. Quantitative studies of the growth of mouse embryo cells in culture and their development into established lines. *J Cell Biol* 1963;17:299–313.
34. Harvey M, Sands AT, Weiss RS, et al. *In vitro* growth characteristics of embryo fibroblasts isolated from p53-deficient mice. *Oncogene* 1993;8:2457–67.
35. Steinman HA, Burstein E, Lengner C, et al. An alternative splice form of Mdm2 induces p53-independent cell growth and tumorigenesis. *J Biol Chem* 2004;279:4877–86.
36. Lee EY, Chang CY, Hu N, et al. Mice deficient for Rb are nonviable and show defects in neurogenesis and haematopoiesis. *Nature* 1992;359:288–94.
37. Clarke AR, Maandag ER, van Roon M, et al. Requirement for a functional Rb-1 gene in murine development. *Nature* 1992;359:328–30.
38. Nikitin AY, Lee WH. Early loss of the retinoblastoma gene is associated with impaired growth inhibitory innervation during melanotroph carcinogenesis in Rb^{+/−} mice. *Genes Dev* 1996;10:1870–9.
39. Hu N, Gutschmann A, Herbert DC, et al. Heterozygous Rb-1 δ 20/+mice are predisposed to tumors of the pituitary gland with a nearly complete penetrance. *Oncogene* 1994;9:1021–7.
40. Harrison DJ, Hooper ML, Armstrong JF, et al. Effects of heterozygosity for the Rb-1t19neo allele in the mouse. *Oncogene* 1995;10:1615–20.
41. Williams BO, Schmitt EM, Remington L, et al. Extensive contribution of Rb-deficient cells to adult chimeric mice with limited histopathological consequences. *EMBO J* 1994;13:4251–9.
42. Maandag EC, van der Valk M, Vlaar M, et al. Developmental rescue of an embryonic-lethal mutation in the retinoblastoma gene in chimeric mice. *EMBO J* 1994;13:4260–8.
43. Hinton DR, Hahn JA, Weiss MH, et al. Loss of Rb expression in an ACTH-secreting pituitary carcinoma. *Cancer Lett* 1998;126:209–11.
44. Tsikitis M, Zhang Z, Edelman W, et al. Genetic ablation of cyclin D1 abrogates genesis of rhabdoid tumors resulting from Ini1 loss. *Proc Natl Acad Sci U S A* 2005;102:12129–34.
45. Imbalzano AN, Jones SN. Snf5 tumor suppressor couples chromatin remodeling, checkpoint control, and chromosomal stability. *Cancer Cell* 2005;7:294–5.
46. Harvey M, Vogel H, Lee EY, et al. Mice deficient in both p53 and Rb develop tumors primarily of endocrine origin. *Cancer Res* 1995;55:1146–51.
47. Park MS, Rosai J, Nguyen HT, et al. p27 and Rb are on overlapping pathways suppressing tumorigenesis in mice. *Proc Natl Acad Sci U S A* 1999;96:6382–7.
48. Tsai KY, MacPherson D, Rubinson DA, et al. ARF mutation accelerates pituitary tumor development in Rb^{+/−} mice. *Proc Natl Acad Sci U S A* 2002;99:16865–70.
49. Hill DA, Chiosea S, Jamaluddin S, et al. Inducible changes in cell size and attachment area due to expression of a mutant SWI/SNF chromatin remodeling enzyme. *J Cell Sci* 2004;117:5847–54.
50. Bruder CE, Dumanski JP, Kedra D. The mouse ortholog of the human SMARCB1 gene encodes two splice forms. *Biochem Biophys Res Commun* 1999;257:886–90.